Spiking Response Model for Uniaxial Carbon Concrete Experimental Data

Ferenc Leichsenring
Institute for Structural Analysis
Technische Universität Dresden
Germany, Dresden 01062
Email: ferenc.leichsenring@tu-dresden.de

Wolfgang Graf
Institute for Structural Analysis
Technische Universität Dresden
Germany, Dresden 01062
wolfgang.graf@tu-dresden.de

Michael Kaliske
Institute for Structural Analysis
Technische Universität Dresden
Germany, Dresden 01062
michael.kaliske@tu-dresden.de

***Abstract*—In engineering related tasks, multiple types of neural networks are common methods of solution. Beside the different kinds of artificial neural networks, spiking neural networks (SNN) represent a continuative development in information processing within the computational units of a net. The properties of this neural type is utilized in this contribution in order to evaluate a uniaxial tension test of carbon reinforced specimen regarding the appearance of cracks in the composite structure during the experiment. The crack detection is considered as showcase for further development of evaluation methods based on SNNs with the focal point to engineering related experiments. This contribution is divided into five main parts, whereas the initial brief introduction is devoted to give an overview of neural networks and their computational units, particularly with regard to the classification of spiking neural networks. Since the proposed application of SNNs targets the evaluation of experimental data – especially crack detection – the uniaxial tension test of carbon reinforced concrete specimen is introduced, which is the basis for the experimental data. The utilized spike response model (SRM) is further presented in order to conclusively apply the method to experimental data for the purpose of crack occurrence detection within the data.**

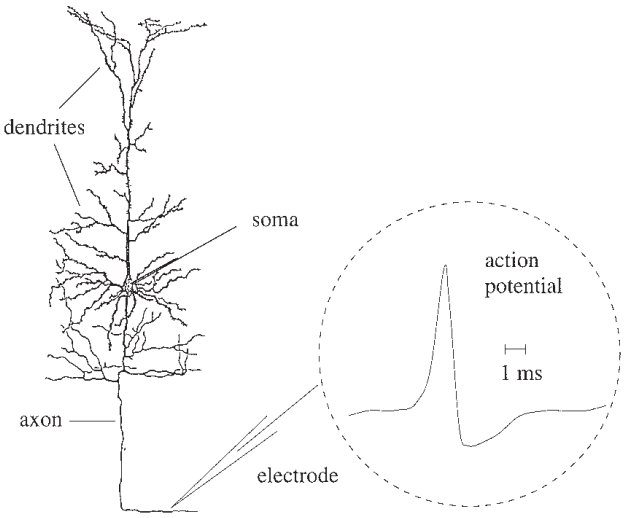

Fig. 1: Drawing of neural components [3]

I. Introduction

Neurons, in their biological form fulfil highly complex tasks. In order to copy this capability artificial neural networks (ANN) with different layouts of the network itself as well as varying neural types have been developed. Over the time they evolved to more powerful and biological realistic models and become efficient computational tools. Due to the generally improved understanding of the brain and its modes of information processing, multiple networks, e.g. feed-forward neural networks (FNN), radial basis function neural networks (RBFN), self organizing maps (SOM), probabilistic or complex valued neural networks are developed for certain tasks. Consequently the scope of application includes pattern recognitions, function approximation, optimization tasks as well as classification problems [1].

In order to classify the used spiking neural networks (SNN, often referred to as pulsed neural networks PNN) into the numerous ANNs, the classification based on their related computational units according to [2] is further introduced.

Basically three different generations can be distinguished. The fist generation is based on *McCulloch-Pitts* neurons as the core unit. Characteristic for this neuron type, as well as derivations such as e.g. *Hopfield* nets or *Boltzmann* machines, is the solely comprehend binary input and output. Hence, they become universal for computations regarded to digital inputs as well as outputs.

Second generation networks are based on computational units featured with an activation function (e.g. sigmoid function). Contrary to first generation neural networks, computations of a continuous set of output values are possible as a result of e.g. weighted sums or polynomials of input values. Representatives are FNN or recurrent sigmoidal neural networks (RNN), which are applicable for time dependent tasks. Evidently second generation nets are able to compute functions with analog input and output values, therefore they are applicable for computations whereas any continuous function with a compact domain and range can be approximated arbitrary well with a single hidden layer. Additionally networks of this type are able to support learning algorithms which are based on gradient descent techniques. An overview regarding possible fields of application in structural analysis is summarized in [4].

Regarding the subjective classification, SNNs are assumed as the consequently third generation of neural nets. As further described in [2], [3], [5], [6] SNNs mimics the information

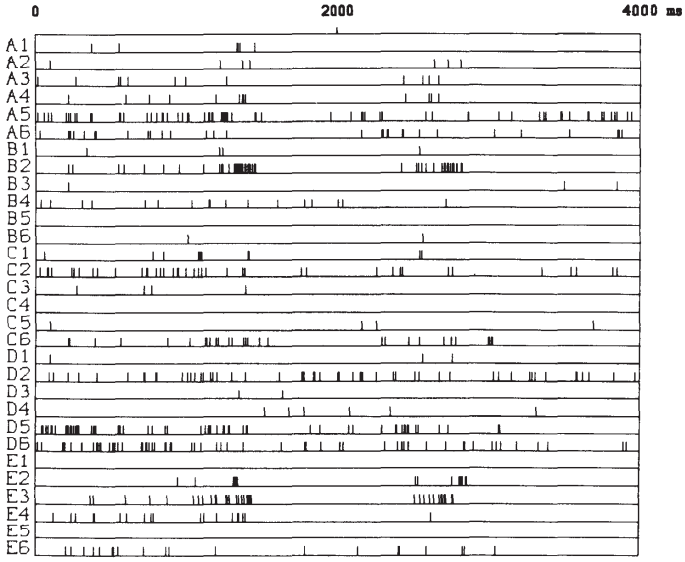

Fig. 2: Simultaneous recordings of firing times of 30 neurons from monkey striate cortex [6]

transfer in biological neurons, via precise timing of spikes or sequences of these. The basic principle of SNNs consists in the consideration of information encoding via the temporal dimension. As depicted in Fig. 1 a biological neuron can be divided into three components. In order of information transmission, the components are denoted as dendritic tree, soma and axon. According to [3], roughly speaking, signals from neuron to neuron, arrive at the dendritic tree and further transmitted to the soma and eventually to the axon. Especially the transition zone between the soma and the axis is of special significance for SNNs. If the total excitation caused by the input is sufficient, an output signal is emitted which is propagated along the axon and distributed to further neurons by its branches, as briefly described in [3]. Due to the temporal resolution SNNs present a large potential solving complex time-dependent tasks by reason of the inherent dynamic representation. As prior mentioned second generation ANN somehow respect the biological idea of the firing rate by means of e.g. the sigmoid function. According to [2] this rate coding interpretation become questionable. Considering the temporal dimension in information encoding in SNNs yields to new insights into brain dynamics and could result in compact representation of large scale neural networks. Experimental evidence indicates that many biological neural systems use the actual timing of single action potentials (further referred to as spikes) to encode information. Studies from e.g. [5] and [6] present the visualization of signal occurrences in a monkeys striate cortex (spike trains, see Fig. 2). Consequently this results lead to the investigation of a third generation of neural networks which employs spiking neurons as an additional computational unit.

This contribution comprehends the application of SNNs to detect crack appearances within provided experimental data, in order to develop an efficient as well as adjustable experiment evaluation system for multiple experiment modes. Therefore it is subdivided into a short introduction to the performed experiment, followed by the utilized theory of spike response models and conclusively the application to experimental data.

II. Uni-axial carbon concrete tension test

In order to capture structural behaviour and determine characteristic material properties, it is necessary to perform suitable structural tests. An uniaxial tension stress test with carbon reinforced concrete is utilizied for crack detection with SNNs. As further described in [7], [8], the test setup is developed to emphasize characteristic material parameters for the new composite material. Therefore a homogeneous uniaxial stress state is induced in the specimen. In Fig. 3 the test setup used to obtain the stress strain dependency is depicted, whereas the over all specimen length is $l = 800\,mm$. The gauge length itself shall be considered as undermentioned, and is therefore from no interest for the SNN based determination of crack appearance. Depending on the material composition, especially the stiffness ratio E_{tex} (Young's modulus of carbon reinforcement) to E_c (Young's modulus of concrete), major cracks occur at the transition from compound load bearing to load bearing solely by the reinforcement. To compare, and eventually deduce uniform characteristic material properties, as equal considered tests are foundation for ultimate state parameters such as ultimate strength as well as strain. Characteristic strength $f_{(\cdot)}$ and stiffness ratios $E_{(\cdot)}$ of the experiment specimen are listed in Tab. I. An automatic determination of cracks (based on existing data or while actual specimen testing) is considered as supportive for future evaluation methods and structural analysis.

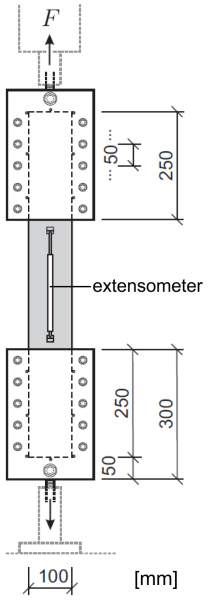

Fig. 3: Uniaxial tension test of carbon reinforced concrete specimen [7]

reinforcement parameters		concrete parameters	
E_{tex}	142000 N/mm^2	E_c	$\geq$ 25000 N/mm^2
$f_{t,tex}$	2940 N/mm^2	$f_{c,c}$	$\geq$ 80 N/mm^2

TABLE I: Characteristic specimen parameters

III. Basic principles of spiking neural networks

Regarding [1], several studies of the cortical pyramidal neurons have shown, the timing of individual spikes as a mode of information encoding is very important in various biological neural networks. Generally, a presynaptic neuron communicates with a postsynaptic neuron by means of trains of spikes or respectively action potentials. In the biological representatives, spikes have a fixed morphology and amplitude. From [2], [3], [9], [10] two options of information transmission encoding are known. Either the transmitted information is encoded in the frequency of spikes (rate coding) or in the timing of spikes (pulse coding). The latter option is considered as more powerful in terms of the wide range of information that may be encoded by the same number of neurons. Therefore pulse coding is utilized for the crack detection application. For the sake of simplicity the mathematical abstraction avoids the modeling of an actual spike train (in biological manner). The firing state is simply coded as binary output of a presynaptic neuron. For fire state the output returns the values 1 or 0 otherwise, at a certain time $t^{(f)}$, whereas the temporal dimension contains the actual analog data. As further detailed described in [2], [3] the later used mathematical formulation of the neural processes is a simplified model that focuses just on few aspects of a biological neuron.

The following utilized type of SNN is called *spike response models* (SRM, see [10], [11]), and adopted to the purpose of crack detection. It is a simplified derivative of the *Hudgkin Huxley* model. Subscripts i, j are used to define the unidirectional relations between a neuron i and presynaptic neurons j. In case of a network structure a set of presynaptic neurons Γ_i is defined as

$$\Gamma_i = \{j \mid \text{presynaptic to } i\} \, . \tag{1}$$

In the utilized SRM, which assumes that a neuron i fires whenever its state variable u_i reaches a certain threshold ϑ. Evidently, the moment of crossing the threshold equals the firing time $t_i^{(f)}$, resulting in the spike train for neuron i

$$\mathcal{F}_i = \{t_i^{(1)}, \ldots, t_i^{(n)}\} \tag{2}$$

The internal state variable u_i represents the membrane potential (electric potential difference) of a certain neuron in terms of a biological representation. One constraint to the fire mechanism is the prescribed positive monotonic behaviour while crossing the threshold. Consequently Eq. (2) becomes

$$\mathcal{F}_i = \{t \mid u_i(t) = \vartheta \ \wedge \ u_i'(t) > 0\} \, . \tag{3}$$

After a spike is triggered, a sequence of events is initiated in biological original. Ion channels open and close, ions flow through the cell membrane into neuron itself, others flow out.

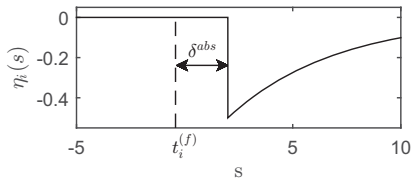

Fig. 4: Kernel function Eq. (4) of neuron i

In terms of the state variable u_i, a sharp peak of the voltage followed by a long lasting negative after potential (spike after potential SAP) occurs.

In the numerical case, the generic time course will be described in the used model by a kernel function $\eta_i(s)$ (neural refractoriness), where $s = t - t_i^{(f)} > 0$ is equal to the elapsed time since the crossing of the state variable at $t_i^{(f)}$. The applied kernel function in this contribution

$$\eta_i(s) = -\xi \exp\left(-\frac{s - \delta^{abs}}{\tau_{m,i}}\right) \mathcal{H}(s - \delta^{abs}) \, , \tag{4}$$

is shown in Fig. 4. Hereby the Heavyside step function is denoted by $\mathcal{H}$, which is defined as

$$\mathcal{H}(s) = \begin{cases} 0 \ \forall \ s \leq 0 \\ 1 \ \forall \ s > 0 \end{cases} \, . \tag{5}$$

In [3], [10], [11] the term $\mathcal{K}\mathcal{H}(s)\mathcal{H}(s - \delta^{abs})$ is subtracted to Eq. (4) in order to model the absolute and negative refractoriness, whereas in this contribution this part is neglected. Despite the missing expression, δ^{abs} is used in favour of numerical stability by inducing a delay between the firing time $t_i^{(f)}$ and the actual refractory period of the neuron, which duration is controlled by the constant $\tau_{m,i}$. This spike event itself is transmitted to other postsynaptic neurons.

Each neuron responses to the spike trains of presynaptic neurons $\mathcal{F}_j$. This voltage response is specified by a function $\varepsilon_{ij}(s)$, whereas $s = t - t_j^{(f)}$ denotes likewise the elapsed time since presynaptic spike occurrence. For each neuron the response to a spike can be either excitatory (excitatory postsynaptic potential, EPSP) or equally inhibitory (inhibitory postsynaptic potential, IPSP). For this cases the membrane potential is either lowered or raised by $\varepsilon_{ij}(s)$. In this contribution only EPSP is used in the form

$$\begin{aligned} \varepsilon_{ij}(s) = \Bigg[& \exp\left(-\frac{s - \delta_{ax}}{\tau_{m,j}}\right) - \\ & - \exp\left(-\frac{s - \delta_{ax}}{\tau_s}\right) \Bigg] \mathcal{H}(s - \delta_{ax}) \, . \end{aligned} \tag{6}$$

As shown in Fig. 5, δ_{ax} defines the delay of the EPSP regarding $t_j^{(f)}$. An axonal transmission delay is respected by δ_{ax}, which originates from the actual transmission through the biological axon (see Fig. 1). Again, the constant $\tau_{m,j}$ manages the duration of the excitatory potential, where the shape is controlled by τ_s. In the neuron itself, all contributions such as the internal spike firing or response to presynaptic spike trains is summed up to the neural state variable (membrane

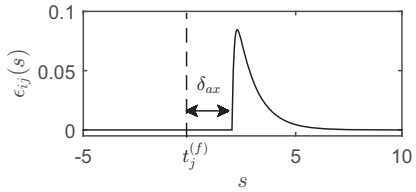

Fig. 5: Excitatory postsynaptic potential, see Eq. (6)

potential) u_i.
Therefore u_i is given by the linear superposition of all contributions as

$$u_i(t) = \sum_{t_i^{(f)} \in F_i} \eta_i \left(t - t_i^{(f)}\right) + \\ + \sum_{j \in \Gamma_i} \sum_{t_j^{(f)} \in F_j} w_{ij} \varepsilon_{ij} \left(t - t_j^{(f)}\right). \tag{7}$$

Since this contribution describes the application for only one sensor, which is considered as presynaptic neuron, the network conclusively consists of only one firing neuron. Hence, the weight is $w_{12} = 1$ and the membrane potential simplifies for this particular evaluation to

$$u(t) = \eta \left(t - t_i^{(f)}\right) + \varepsilon \left(t - t_j^{(f)}\right). \tag{8}$$

An section of an exemplary tensile data is encoded by pulse coding (described further on) and evaluated by a single spiking neuron. In Fig. 6, the state variable u_i as well as the spike train $\mathcal{F}_j$ is depicted.

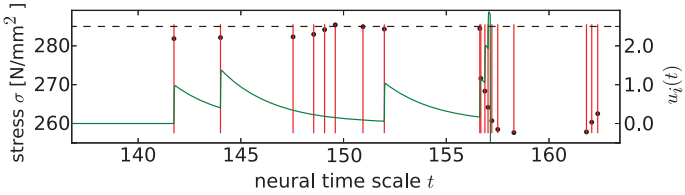

Fig. 6: Encoded experimental data points (black dots), spike train (red) and related internal state variable $u_i(t)$ (green)

IV. Application to data samples

To determine the cracks during the experiment, the either real time recorded machine data or an existing data set of is presumed as presynaptic spike train $\mathcal{F}_j$. The specimen test (see Section II) is displacement driven with a constant displacement increment $w = 0.015\,mm$. The measured force is used as the criteria property in terms of crack detection. External displacement is in equilibrium with internal stresses, which are captured by the recorded force F (compare Fig. 3). Crack mechanics shall be neglected in this contribution, nevertheless provides [12] a comprehensive summary of possible crack modes and related mechanics. In case of a crack of concrete at a certain point, the stiffness ratio of the reinforcement $E_{tex} < E_{composite}$ leads to a larger strain (crack opening) and to a decreased measurable force, compared to an intact state (uncracked stress state) of the specimen. First attempts to detect cracks by e.g. evaluation of distribution of force jumps within a data set, lead to a not significant threshold in order to distinguish cracks. Aiming to a general method, less dependent to testing machines (measure frequency) and specimen size, a more adoptable method with use of a single spiking neuron has been developed.

parameter	value	parameter	value
δ^{abs}	0.1	τ_s	0.009
δ_{ax}	0.1	ξ	0.5
$\tau_{m,i}$	10	ϑ	2.5
$\tau_{m,j}$	2.5		

TABLE II: Parameter set of spiking neuron

The data is transformed to the temporal dimension via pulse coding. For a given experimental data set of stress data $\underline{\sigma} = [\sigma_1, \ldots, \sigma_{n_s}]$, an additional data set is created storing consecutive increments $\underline{\sigma}_\Delta = [\sigma_{\Delta,1}, \ldots, \sigma_{\Delta,i}, \ldots, \sigma_{\Delta,n_s-1}]$, with $\sigma_{\Delta,i} = \sigma_{i+1} - \sigma_i$. The resulting firing times of the presynaptic spike train $\mathcal{F}_j = \{t_j^{(1)}, \ldots, t_j^{(n_s-1)}\}$ are determined by

$$t_j^{(k)} = \frac{\max[\underline{\sigma}_\Delta]/\kappa_t}{\sigma_{\Delta,k}}, k = 1, \ldots, n_s - 1\,. \tag{9}$$

However, the temporal coding of the information can be assumed as inverse to the actual physical behaviour, since large difference is represented by a minor time gap between the spikes. The visual representation of the pulse encoding is shown in Fig. 7b) and in the coded state Fig. 7c). This encoded section is associated to the original section of the stress strain dependency depicted in Fig. 7a). As the figures clarify, the obvious crack is respected in the high pulse rate at approx. $t > 150$ (see Fig. 7c)).
In use of the neural parameter shown in Table II the equivalent state variable for an section of a exemplary experimental data is shown in Fig. 8. Due to further constraint

$$\sigma'(t) < 0 \quad \text{or } \sigma_{t_i^{(k)}} - \sigma_{t_i^{(k-1)}} < 0 \tag{10}$$

not every spike yields to an excitory postsynaptic potential (compare Fig. 6). Finally, four major peaks, each greater then the selected threshold ϑ, lead to resulting firing times $\mathcal{F}_i = \{5, 55, 206, 270\}$ (decoded to consecutive index). Inherent to the method is firing of the single neuron equal to appearance of a crack, therefore the decoded firing times are shown for each scale (consecutive index and strain) in Fig. 9 as well as Fig. 10. Since the evaluation of a tensile test, regarding the count of crack appearance, sporadically is carried out in a visual evaluation, minor cracks tend to be neglected in favour of comparably major cracks. Therefore the crack detection for considerably large cracks is assumed as adequate.

V. Conclusion and outlook

Within this contribution the basic principles of SNN are mentioned and the spike response model is adopted in order to detect cracks within structural tensile experimental data of

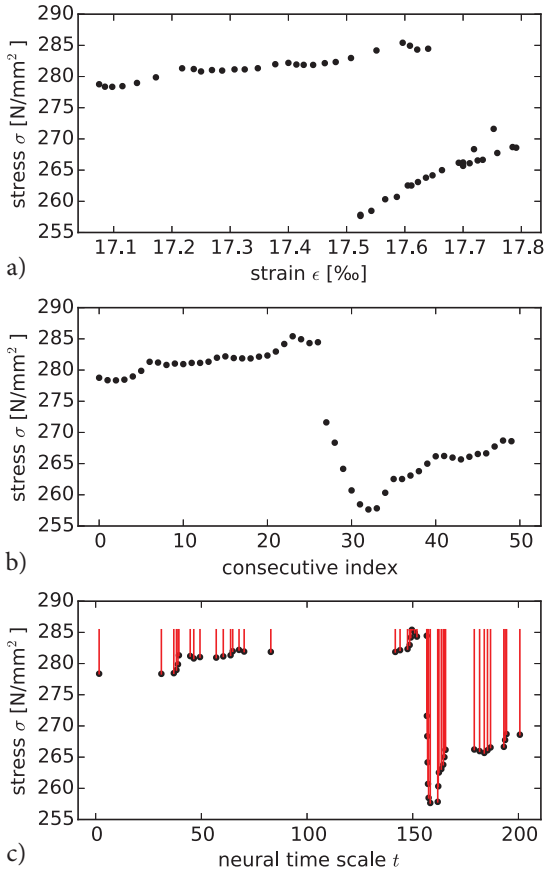

Fig. 7: a) Original stress strain dependency
b) Stress over consecutive index
c) Stress spike train after temporal encoding

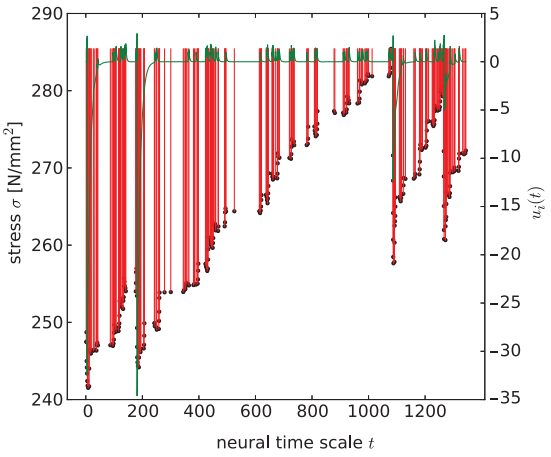

Fig. 8: Spike train $\mathcal{F}_j$ and the corresponding state variable $u_i(t)$

carbon reinforced concrete specimens. Hereby pulse coding is utilized to decode the data to a temporal dimension. The neurons internal state variable only responses to an excitatory postsynaptic potential to presynaptic spike trains (real time sensor data or data set). In terms of the application to actual

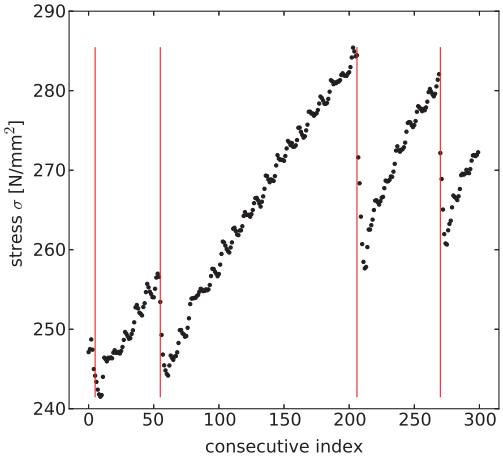

Fig. 9: Detected cracks regarding to the consecutive index

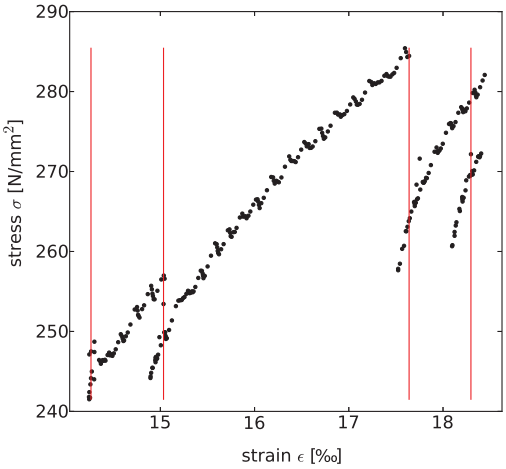

Fig. 10: Detected cracks with the strain stress dependency

test data, evidently major cracks within the data could be identified. The method is adjustable to the crack size only with variation of three constants $\vartheta, \tau_{m,i}, \tau_{m,j}$ and therefore becomes simply adaptable to different testing environments as well as evaluation tasks. In principle, further developments could result to a network structure of spiking neurons considering multiple requirements of the data evaluation by construction of a neural net for different sensor types or equivalent input dimensions. In theory the proposed method is capable of real time crack detection, hence testing situations which require appearance of initial cracks could be designed independently from human interaction and subjective interpretation.

Acknowledgment

The actual testing of carbon concrete specimens at *Institut für Massivbau, TU Dresden*, and conclusively the provided data for this contribution has been carried out within the *Zwanzig20* project *Carbon Concrete Composite* (C^3) founded by *Bundesministerium für Bildung und Forschung (BMBF)*. We'd like to thank the mentioned institutions for their support.

REFERENCES

[1] S. Ghosh-Dastidar and H. Adeli, "Spiking neural networks", *International Journal of Neural Systems*, vol. 19, pp. 295–308, Aug 2009.

[2] W. Maass, "Networks of spiking neurons: The third generation of neural network models", *Neural Networks*, vol. 10, pp. 1659–1671, Dec 1997.

[3] W. Maass, *Pulsed neural networks*. Cambridge, Mass: MIT Press, 1999.

[4] W. Graf, J.-U. Sickert, S. Freitag, S. Pannier, and M. Kaliske, "Neural network approaches in structural analysis considering imprecision and variability", in *Soft Computing Methods for Civil and Structural Engineering*, Stirlingshire: Saxe-Coburg Publ., pp. 59–85, 2011.

[5] D. Perrett, E. Rolls, and W. Caan, "Visual neurones responsive to faces in the monkey temporal cortex", *Experimental Brain Research*, vol. 47, Sep 1982.

[6] J. Krüger and F. Aiple, "Multi-microelectrode investigation of monkey striate cortex: Link between correlational and neuronal properties in the infragranular layers", *Vis. Neurosci.*, vol. 5, p. 135, Aug 1990.

[7] A. Scholzen, *Flächige Tragstrukturen aus textilbewehrtem Beton: Experimentelle und numerische Charakterisierung des Tragverhaltens, Bemessung und Herstellungsmethodik*. RWTH Aachen, 2015.

[8] E. Schütze, E. Lorenz, and M. Curbach, "Test methods for textile reinforced concrete", in *FERRO-11 – 11th International Symposium on Ferrocement and 3rd ICTRC – International Conference on Textile Reinforced Concrete*, RILEM Publications SARL, 2015.

[9] S. O. Haykin, *Neural Networks and Learning Machines (3rd Edition)*. McMaster University: Pearson, 2008.

[10] W. Gerstner, "Time structure of the activity in neural network models", *Phys. Rev. E*, vol. 51, pp. 738–758, Jan 1995.

[11] W. M. Kistler, W. Gerstner, and J. L. v. Hemmen, "Reduction of the Hodgkin-Huxley equations to a single-variable threshold model", *Neural Computation*, vol. 9, pp. 1015–1045, Jul 1997.

[12] T. L. Anderson, *Fracture Mechanics: Fundamentals and Applications, Third Edition*. London: CRC Press, 2004.